

# Reactive oxygen species produced by myeloid cells in psoriasis as a potential biofactor contributing to the development of vascular inflammation

Theresa Schaller<sup>1</sup>  | Julia Ringen<sup>2,3</sup>  | Berenice Fischer<sup>4</sup> |  
 Tabea Bieler<sup>5,6</sup>  | Katharina Perius<sup>2,3</sup> | Tanja Knopp<sup>2,3,7,8</sup> |  
 Katharina S. Kommos<sup>5,9</sup>  | Thomas Korn<sup>10,11</sup> | Mathias Heikenwälder<sup>5,12</sup> |  
 Matthias Oelze<sup>2,13</sup> | Andreas Daiber<sup>2,13</sup> | Thomas Münzel<sup>2,3,13</sup> |  
 Daniela Kramer<sup>4</sup> | Philip Wenzel<sup>2,3,13</sup> | Johannes Wild<sup>2,3,13</sup>  |  
 Susanne Karbach<sup>2,3,13</sup>  | Ari Waisman<sup>1,14</sup> 

<sup>1</sup>Institute for Molecular Medicine, University Medical Center of the Johannes Gutenberg-University Mainz, Mainz, Germany

<sup>2</sup>Department of Cardiology – Cardiology I, University Medical Center of the Johannes Gutenberg-University Mainz, Mainz, Germany

<sup>3</sup>Center of Thrombosis and Hemostasis (CTH), University Medical Center of the Johannes Gutenberg-University Mainz, Mainz, Germany

<sup>4</sup>Department of Dermatology, University Medical Center of the Johannes Gutenberg-University Mainz, Mainz, Germany

<sup>5</sup>Division of Chronic Inflammation and Cancer, German Cancer Research Center (DKFZ), Heidelberg, Germany

<sup>6</sup>Interdisciplinary Center for Scientific Computing (IWR), University of Heidelberg, Heidelberg, Germany

<sup>7</sup>Department of Hematology and Central Hematology Laboratory, Inselspital University Hospital Bern, Bern, Switzerland

<sup>8</sup>Department of Clinical Research, University of Bern, Bern, Switzerland

<sup>9</sup>Department of Dermatology, University of Heidelberg, Heidelberg, Germany

<sup>10</sup>Institute for Experimental Neuroimmunology, Technical University of Munich School of Medicine, Munich, Germany

<sup>11</sup>Munich Cluster for Systems Neurology (SyNergy) Ludwig-Maximilians-University Munich, Munich, Germany

<sup>12</sup>The M3 Research Institute, Eberhard Karls University Tübingen, Tübingen, Germany

<sup>13</sup>German Center for Cardiovascular Research (DZHK) – Partner Site Rhine-Main, University Medical Center of the Johannes Gutenberg-University Mainz, Mainz, Germany

<sup>14</sup>Research Center for Immunotherapy, Johannes Gutenberg-University Mainz, Mainz, Germany

## Correspondence

Susanne Karbach, Department of Cardiology, Thrombosis and Hemostasis, University Medical Center of the Johannes Gutenberg-University Mainz,

## Abstract

Psoriasis is an immune-mediated inflammatory skin disease driven by interleukin-17A (IL-17A) and associated with cardiovascular dysfunction. We used a severe psoriasis mouse model of keratinocyte IL-17A overexpression

**Abbreviations:** Cxcl2, chemokine (C-X-C motif) ligand 2; IL-1 $\beta$ , interleukin-1 $\beta$ ; IL-17A, interleukin-17A; Mpo, myeloperoxidase; Elane, neutrophil elastase; Nrf2, nuclear factor erythroid 2-related factor 2; n.d., not determinable; PDBu, phorbol-12,13-dibutyrate; ROS, reactive oxygen species; S100a9, S100 calcium-binding protein A9; Sod, superoxide dismutase; Scl41a3, solute carrier family 41, member 3; LN, lymph node; TNF $\alpha$ , tumor necrosis factor-alpha.

Theresa Schaller, Julia Ringen, Johannes Wild, Susanne Karbach, and Ari Waisman contributed equally to this study.

This is an open access article under the terms of the [Creative Commons Attribution-NonCommercial-NoDerivs](https://creativecommons.org/licenses/by-nc-nd/4.0/) License, which permits use and distribution in any medium, provided the original work is properly cited, the use is non-commercial and no modifications or adaptations are made.

© 2023 The Authors. *BioFactors* published by Wiley Periodicals LLC on behalf of International Union of Biochemistry and Molecular Biology.

Langenbeckstr. 1, Mainz 55131, Germany.  
Email: karbasu@uni-mainz.de

### Funding information

Boehringer Ingelheim Stiftung;  
Bundesministerium für Bildung und  
Forschung, Grant/Award Numbers:  
BMBF 01EO1503, BMBF EDU-V24;  
Deutsche Forschungsgemeinschaft,  
Grant/Award Number: KA 4035/1-1;  
Deutsche Herzstiftung; DFG,  
Grant/Award Numbers: TRR156/2  
(ID246807620), SFB1054(ID210592381),  
TRR128(ID213904703), TRR274  
(ID408885537), TRR355(ID490846870),  
EXC2145(ID390857198), TRR355/1  
(490846870); DZHK Excellence  
Programme; Else-Kröner-Fresenius  
Foundation; Hertie Network of Clinical  
Neuroscience; Peter-Hans Hofschneider  
Foundation; Physician-Scientist  
Programme of Heidelberg University;  
University of Mainz (Inneruniversitäre  
Forschungsförderung); Ministry of Science  
Baden-Württemberg; Munich Cluster for  
Systems Neurology

(K14-IL-17A<sup>ind/+</sup>, IL-17A<sup>ind/+</sup> control mice) to investigate the activity of neutrophils and a potential cellular interconnection between skin and vasculature. Levels of dermal reactive oxygen species (ROS) and their release by neutrophils were measured by lucigenin-/luminol-based assays, respectively. Quantitative RT-PCR determined neutrophilic activity and inflammation-related markers in skin and aorta. To track skin-derived immune cells, we used PhAM-K14-IL-17A<sup>ind/+</sup> mice allowing us to mark all cells in the skin by photoconversion of a fluorescent protein to analyze their migration into spleen, aorta, and lymph nodes by flow cytometry. Compared to controls, K14-IL-17A<sup>ind/+</sup> mice exhibited elevated ROS levels in the skin and a higher neutrophilic oxidative burst accompanied by the upregulation of several activation markers. In line with these results psoriatic mice displayed elevated expression of genes involved in neutrophil migration (e.g., *Cxcl2* and *S100a9*) in skin and aorta. However, no direct immune cell migration from the psoriatic skin into the aortic vessel wall was observed. Neutrophils of psoriatic mice showed an activated phenotype, but no direct cellular migration from the skin to the vasculature was observed. This suggests that highly active vasculature-invading neutrophils must originate directly from the bone marrow. Hence, the skin-vasculature crosstalk in psoriasis is most likely based on the systemic effects of the autoimmune skin disease, emphasizing the importance of a systemic therapeutic approach for psoriasis patients.

### KEYWORDS

interleukin-17A, neutrophil granulocytes, psoriasis, reactive oxygen species

## 1 | INTRODUCTION

Psoriasis is an interleukin-17A (IL-17A) and IL-23 driven autoimmune skin disease mediated by the adaptive and innate immune system.<sup>1,2</sup> This chronic inflammatory state affects 2%–3% of the world population.<sup>3,4</sup> Its classic histological features are thickened epidermis resulting from hyperproliferation of keratinocytes and altered differentiation of keratinocytes combined with infiltration of myeloid cells into the dermal layer.<sup>1,5,6</sup> Besides skin inflammation, severe chronic psoriasis is associated with several comorbidities like psoriatic arthritis, metabolic syndrome, cardiovascular disease (CVD), and non-alcoholic fatty liver disease (NAFLD).<sup>7–9</sup> The inflammatory skin disease was found to be an independent risk factor for CVD and not only secondary due to the increased occurrence of classical cardiovascular risk factors in psoriasis.<sup>10</sup> Indeed, psoriasis patients have a 57% higher probability of dying from a cardiovascular event compared to the general population.<sup>10,11</sup> On a cellular and molecular level, the cytokines IL-17A and IL-17F produced by T cells and innate immune cells were identified as key players in

the pathology of psoriasis.<sup>12–14</sup> Reactive oxygen species (ROS)-activated proinflammatory signals in the skin are of crucial relevance in the immunoregulation of psoriasis contributing to inflammatory cell recruitment and thus intensifying the inflammatory cascade.<sup>15,16</sup> Both myeloid cells and keratinocytes are sources of oxidative stress formation in the skin.<sup>16</sup> In the vasculature, oxidative stress leads to vascular dysfunction and has an important prognostic implication for subsequent cardiovascular events.<sup>17</sup>

Besides the endothelial cells, myeloid cells invading into the vessel wall present a relevant ROS source in the vasculature contributing to the progress of vascular inflammation and atherosclerosis.<sup>18–20</sup> Oxidative stress formation is understood to have a key role in CVD development in psoriasis patients linking skin and vascular disease.<sup>21</sup> We could show that dermal overexpression of IL-17A which results in a severe chronic psoriasis-like skin inflammation (K14-IL-17A<sup>ind/+</sup> psoriatic mice, IL-17A<sup>ind/+</sup> control mice) is associated with a significant vascular dysfunction.<sup>22</sup> The vascular phenotype was connected to the infiltration of immune cells – majorly neutrophils – and increased ROS

formation in the aortic vessel wall.<sup>23</sup> This corroborates data from the murine model of angiotensin II (AngII) induced arterial hypertension, in which the ROS-producing myeloid cells contribute to the development of hypertension and vascular dysfunction.<sup>19</sup> Of note, patients with severe psoriasis display vascular inflammation in multiple segments of the aorta.<sup>24</sup> Non-calcified plaque burden in coronary arteries in psoriasis patients assessed by coronary computed tomography angiography was described to correlate with skin disease severity.<sup>25</sup> Under biologic therapy for moderate to severe psoriasis, coronary inflammation decreased in parallel.<sup>26</sup> In total, this hints towards a correlation between skin disease severity with the degree of vascular involvement.<sup>27</sup> Being aware of psoriasis as a cardiovascular risk factor and of the life-limiting cardiovascular comorbidity in psoriasis patients is of highest clinical importance to improve patient care.<sup>28,29</sup>

To date, the mechanistic underpinnings between psoriatic skin inflammation and the associated cardiovascular dysfunction are lacking. Invading myeloid cells producing ROS and pro-inflammatory cytokines could be a possible linking factor between skin and vascular inflammation. This work aims to analyze neutrophils and neutrophil activity and further to elucidate the skin-vascular crosstalk in severe chronic murine psoriasis. We aimed to especially answer the question if inflammatory ROS-producing cells migrate directly from the psoriatic plaque to the vasculature or whether indirect and systemic effects of the inflammatory circuits drive cardiovascular comorbidity in psoriasis.

## 2 | EXPERIMENTAL PROCEDURES

### 2.1 | Mice

All animals were housed in accordance with relevant laws and institutional guidelines of the Central Animal Facility of the University Medical Center Mainz, Germany. For all experiments mice aged 7–10 weeks with mixed gender were used. Mice were sacrificed in deep isoflurane anesthesia and cervical dislocation. For heart puncture, this method was combined with i.p. injection of Fentanyl (0.05 mg/kg) and Midazolam (5.0 mg/kg). All experiments on mice were conducted after approval by the Animal Care and Use Committee from the Land of Palatine, approval numbers G17-1-076 and G21-1-039.

### 2.2 | Chemicals

All chemicals were of highest analytical grade from the Sigma-Aldrich/Merck unless otherwise stated.

### 2.3 | Mouse model of psoriasis-like skin disease with focus on inflammatory cell migration and scoring

PhAM<sup>Δ/Δ</sup> (excised) mice were crossed to a K14-Cre mouse line, followed by crossing to IL-17A<sup>ind/ind</sup> mice to obtain PhAM<sup>Δ/+</sup>-K14-IL-17A<sup>ind/+</sup> mice = PhAM-K14-IL-17A<sup>ind/+</sup>.<sup>30,31</sup> PhAM<sup>Δ/Δ</sup> mice ubiquitously express the green fluorescent protein mito-Dendra2 in the mitochondria, which photoconverts upon laser illumination ( $\lambda = 405$  nm) into a red fluorescing species.<sup>31</sup> The severity of psoriasis-like skin disease was determined by modified PASI scoring from the age of 5 weeks on.<sup>23</sup> The scores for erythema and scaling of the skin (1 = mild, 2 = intermediate, 3 = severe, 4 = very severe) and percentage of the inflamed skin were determined. The cumulative PASI score was calculated as follows: (erythema score + scaling score)  $\times$  affected area [%]/100. In the manuscript, the cumulative PASI scores are depicted.

### 2.4 | Laser illumination

K14-Cre negative control mice were shaved and depilated (Veet, Slough, UK) on the upper back area 1 day before the illumination. Sick PhAM-K14-IL-17A<sup>ind/+</sup> mice were illuminated directly on the plaque skin. Mice were illuminated by a 405 nm laser (Soliton, Gilching, Germany) on scaled/shaved skin and ears for 4–5 min per area under isoflurane anesthesia.<sup>31</sup> One day after illumination, the mice were sacrificed and analyzed.

### 2.5 | Isolation of neutrophils from whole blood

The venous blood of anesthetized K14-IL-17A<sup>ind/+</sup> or PhAM-K14-IL-17A<sup>ind/+</sup> mice and controls was taken by heart puncture and anticoagulated with EDTA (0.1% v/v). To isolate neutrophils from the whole blood an EasySep™ Mouse Neutrophil Enrichment Kit (STEMCELL Technologies, Vancouver, Canada) was used according to the manufacturer's instructions.

### 2.6 | Flow cytometry analysis

Spleens and lymph nodes (LNs) were mechanically disrupted by pressing them through a 40  $\mu$ m cell strainer (Sarstedt, Nümbrecht, Germany). Erythrocytes of the spleen were lysed with ACK buffer (150 mM NH<sub>4</sub>Cl, 10 mM KHCO<sub>3</sub>, 1 mM Na<sub>2</sub>EDTA·2Na, pH 7.2). Ears were separated into dorsal and ventral parts and transferred

into digestion mix (0.12 mg/ml DNase I (Roche, Basel, Switzerland), 0.25 mg/ml Liberase (Roche) in RPMI-1640 Medium (ThermoFisher Scientific, Waltham, MA)). The tissue was cut into small pieces by scissors and incubated for 1 h at 37°C. The cells were filtered through a 70 µm cell strainer. Aortas were isolated and fatty tissue was removed before the digestion with Liberase (1 mg/ml) for 30 min at 37°C. Subsequently, cells were filtered through 70 µm cell strainer.<sup>23</sup> Single cell suspensions were treated with Fc-Block (BioXCell, Lebanon, NH) and subsequently surface stained with the following monoclonal antibodies: CD11b (clone: M1/70, eBioscience, San Diego, CA), Gr-1 (clone: RB6-8C5, BD Bioscience, Franklin Lakes, NJ), CD45.2 (clone: 104, eBioscience, San Diego, CA), CD19 (clone: 6D5, Biolegend, San Diego, CA) and CD90.2 (clone: 53-2.1, PE, eBioscience, San Diego, CA). Fixable Viability Dye eFluor450 (eBioscience, San Diego, CA) was used to exclude dead cells. The stained cells were fixed in formaldehyde in phosphate-buffered saline (2%) for 30 min at 4°C. All samples were acquired on an Invitrogen™ Attune™ NxT flow cytometer (Thermo Fisher, Waltham, MA) and analyzed using FlowJo software (BD, Franklin Lakes, NJ).

## 2.7 | Flow cytometric analysis of ROS production in blood

We took venous blood of anesthetized K14-IL-17A<sup>ind/+</sup> mice and control mice by heart puncture and anticoagulated it with EDTA (0.1% v/v). Blood samples were treated with or without phorbol-12,13-dibutyrate (PDBu) for 15 min at room temperature, stained with CellROX™ Reagent (deep red, 5 µM, Thermo Fisher Scientific, Waltham, MA) as published by Cossarizza et al.<sup>32</sup> and incubated for 30 min in a water bath at 37°C. For negative controls samples were incubated in the absence of CellROX™ reagent. After a short centrifugation step (10 s), the supernatant was preserved and the cell pellet was stained with the following monoclonal antibodies: CD45-eFluor 506 (Clone: 30-F11; Thermo Fisher, Waltham, MA), CD11b-phycoerythrin-Cyanine 7 (PE-Cy7) (Clone: M1/70; Thermo Fisher, Waltham, MA), Ly6G-super bright 600 (Clone: 1A8; Thermo Fisher, Waltham, MA), Ly6C-peridinin chlorophyll protein (PerCP)-Cy5.5 (Clone: KH1.4; Thermo Fisher, Waltham, MA) and Viability Dye eFluor 780 (Thermo Fisher, Waltham, MA) for 20 min at room temperature. The conserved supernatant was added and samples were diluted (final conc. 1:2000) and immediately analyzed using the Invitrogen™ Attune™ NxT flow cytometer (Thermo Fisher Scientific, Waltham, MA) and the Invitrogen™ Attune™ No-Wash

No-Lyse Filter Kit (Thermo Fisher Scientific, Waltham, MA).

## 2.8 | Detection of reactive oxygen species formation

### 2.8.1 | ROS measurement in the skin with lucigenin

The plaque-affected back skin of K14-IL-17A<sup>ind/+</sup> mice and the healthy back skin of IL-17A<sup>ind/+</sup> controls was isolated and cut into pieces of 1 cm<sup>2</sup> size. These were incubated in PBS for 20 min on a thermocycler at 37°C. To detect the formation of ROS especially superoxide, the skin was added to a vial with lucigenin (5 µM in PBS) and with a tube luminometer (Lumat LB 9507, Berthold Technologies, Sprendlingen, Germany) the lucigenin-enhanced chemiluminescence was measured. After the measurement the skin was allowed to dry completely and was weighed. The results shown here have been weight-adjusted.<sup>33</sup>

### 2.8.2 | ROS measurement in isolated Ly6G<sup>+</sup> neutrophils via chemiluminescence reaction

Neutrophils were isolated from EDTA-anticoagulated whole blood by using the EasySep™ Mouse Neutrophil Enrichment Kit (STEMCELL Technologies, Vancouver, Canada) as described above. The same number of cells (2.5 × 10<sup>5</sup> cells) was used for oxidative burst measurement in neutrophils. Phorbol-12,13-dibutyrate (PDBu) was added to stimulate the formation of an oxidative burst in leukocytes. After the incubation for 10 min the oxidative burst was measured by using the 8-amino-5-chloro-7-phenylpyridol-(3,4-d) pyridazine-1,4-(2H,3H)-dione sodium salt (L-012)-enhanced chemiluminescence as previously described.<sup>33,34</sup> The measured ROS are mostly hydrogen peroxide, which reacts in a peroxidase-catalyzed reaction with L-012 to generate a chemiluminescence signal.<sup>35</sup> Peroxidase activity comes from endogenous enzymes, for example, myeloperoxidase, in the neutrophils. The chemiluminescence was detected by a Spark™ Multimode Microplate Reader (Tecan Trading AG, Männedorf, Switzerland).

## 2.9 | Blood analysis of bone marrow

Bone marrow was isolated from tibia and femur bones of K14-IL-17A<sup>ind/+</sup> or IL-17A<sup>ind/+</sup> controls. The bone

marrow was diluted in PBS and a complete blood cell count was performed with a Vetscan HM5 (Abaxis Europe GmbH, Griesheim Germany).<sup>36</sup>

## 2.10 | Quantitative real time PCR

### 2.10.1 | In skin and aortic tissue

With the help of the TissueLyser II (Qiagen, Hilden, Germany) skin and aortic tissue was pulverized or homogenized to isolate RNA. This was suspended in GIT buffer (4 M guanidinium-isothiocyanate, 25 mM Na-citrat, 0.5% N-lauroylsarcosine, 7.2% mercaptoethanol) and afterwards the RNA was extracted with phenol-chloroform.<sup>37</sup> To measure the RNA concentration a NanoDrop™ spectrophotometer (Thermo Fisher, Waltham, MA) or a Spark™ Multimode Microplate Reader (Tecan Trading AG, Männedorf, Switzerland) was used.<sup>38</sup> With 0.5 µl of total RNA a TaqMan® Gene Expression Assay (Applied Biosystems™, Waltham, MA) was performed as described in the manufacturer's protocol. The following TaqMan® primers were used: C-X-C motif chemokine 2 (*Cxcl2*; Mm00436450\_m1, FAM marked; Thermo Fischer, Waltham, MA) and Nuclear factor erythroid 2-related factor 2 (*Nrf2*; Mm00477784\_m1 (Nfe2l2), FAM-marked; Thermo Fischer, Waltham, MA). The gene expression was normalized to TATA box binding protein (*Tbp*; Mm00446973\_m1, VIC-marked; Thermo Fischer, Waltham, MA) mRNA as an endogenous control. To analyze 1.0 µg of cDNA the QuantiTect SYBR Green RT-PCR was used. To quantify mRNA expression the comparative delta CT method was used. As an endogenous control, the gene expression was normalized to glyceraldehyde 3-phosphate dehydrogenase (*Gapdh*) mRNA. For the QuantiTect-SYBR Green RT-PCRs the following primers were used: S100 calcium-binding protein A9 (*S100a9*, forward 5'-AATGGTGAAGCACAGTTGG-3', reverse 3'-CTGGTTTGTGTCAGGTCCTC-5'), Superoxide dismutase 1 (*Sod1*, forward 5'-AACCAGTTGTGTTGTCAGGAC-3', reverse 3'-CCACATGTTTCTTAGAGTGAGG-5') Superoxide dismutase 2 (*Sod2*, forward 5'-CAGACCTGCCTTACGACTATGG-3', reverse 3'-CTCGGTGGCGTTGAGATTGTT-5'), Superoxide dismutase 3 (*Sod3*, forward 5'-CCTTCTTGTCTACGGCTTGC-3', reverse 3'-TCGCTATCTTCTCAACCAGG-5'), Solute carrier family 41 member 3 (*Scl41a3*, forward 5'-CTCAGCCTTGAGTTCCGCTTT-3', reverse 3'-GCAGGATAGGTATGGCGACC-5'), and glyceraldehyde 3-phosphate dehydrogenase (*Gapdh*, forward 5'-TACCCCAATGTGTCCGTCGTG-3', reverse 3'-CCTTCAGTGGCCCTCATGTC-5').

### 2.10.2 | In isolated Ly6G<sup>+</sup> neutrophils

Neutrophils were isolated from EDTA-anticoagulated whole blood by using the EasySep™ Mouse Neutrophil Enrichment Kit (STEMCELL Technologies, Vancouver, Canada) as described above. The RNA was isolated with the help of a RNeasy Plus Micro Kit (Qiagen, Hilden, Germany) as described in the manufacturer's protocol. After the cDNA synthesis the Maxima™ SYBR Green qPCR Master Mix (Thermo Fischer, Waltham, MA) was used to analyze 2.5 µl of cDNA. The comparative delta CT method was used to quantify the mRNA expression. Relative mRNA levels were normalized to *β-Actin* mRNA as an endogenous control. Afterwards control cells were set to 1 and the relative mRNA induction is calculated of the mRNA levels in control cells (shown as the mean log ratio). The following primer sequences were used: Interleukin 1β (*IL-1b*, forward 5'-AGCTGAAAGCTCTCCACCTC-3', reverse 3'-GCTTGGATCCACACTCTCC-5'), Myeloperoxidase (*Mpo*, forward 5'-GGAGCCCCGGAAGATTGTAG-3', reverse 3'-CGTTGTGAAGACATTGGCG-5'), Neutrophil Elastase (*Elane*, forward 5'-ACCCAGTGTGCTACAAGAGC-3', reverse 3'-GTGCATACGTTACACGACG-5'), Proteinase 3 (*Prtn3*, forward 5'-CAGCTAAACCGGACAGCCTC-3', reverse 3'-GTTCCCGGCATAGGAAGGTG-5'), *Actin* (forward 5'-AGGAGTACGATGAGTCCGGC-3', reverse 3'-GGTGAAAACGCAGCTCAGTA-5').

## 2.11 | Immunohistochemistry

Bone samples were fixed in 4% paraformaldehyde (Carl Roth GmbH + Co. KG, Karlsruhe, Germany) for 48 h at room temperature and transferred to Decalcifier soft (Carl Roth GmbH + Co. KG, Karlsruhe, Germany) for 48–72 h. Completely decalcified bones were paraffin embedded. A 2 µm sections were prepared and stained with Ly6G IHC antibody (BD Bioscience, clone 1A8, 1:800, rat). Incubation in Bond™ Primary Antibody Diluent (Leica Biosystems Nussloch GmbH, Nussloch, Germany) and staining was performed on a BOND-MAX Automated IHC/ISH Stainer (Leica Biosystems Nussloch GmbH, Nussloch, Germany). Slides were scanned using an Aperio AT2 scanner (Leica Biosystems Nussloch GmbH, Nussloch, Germany). Automated counting of Ly6G positive cells was performed on 8–10 representative areas in the bone with QuPath version 0.3.2.<sup>39</sup>

## 2.12 | Statistical analysis

Statistical analysis was performed with GraphPad Prism software (version 9.3.1; GraphPad Software, Inc., San

Diego, CA). Data were tested for outliers identified by using the ROUT method at a stringency of 1% and analyzed for normal distribution using the Kolmogorow–Smirnow test. For normal distribution the unpaired student's *t*-test or the 2-way ANOVA test with Bonferroni post-test was applied. If data were not normally distributed, we performed the Mann–Whitney test as indicated in the figure legends. *P* values of <0.001, <0.01, and <0.05 were considered statistically significant and marked by 3, 2, and 1 asterisks (\*). Data are presented as mean ± SEM.

### 3 | RESULTS

To better understand the inflammatory reaction observed in mice with severe psoriasis, we first measured the levels of ROS species in the skin. We found that the inflamed skin of K14-IL-17A<sup>ind/+</sup> psoriatic mice exhibited significantly increased ROS, or more precisely superoxide, compared to the healthy skin of IL-17A<sup>ind/+</sup> control mice (Figure 1A). This matched the severe skin inflammation due to the IL-17A-driven influx of myeloid cells, as previously described.<sup>22</sup> Further analysis of neutrophil granulocytes isolated from K14-IL-17A<sup>ind/+</sup> mice also showed increased oxidative burst formation upon PDBu stimulation compared with neutrophils isolated from control mice (Figure 1B), confirmed by flow cytometric analysis (Figure 1C). In agreement, we found a significant increase in expression levels of *Neutrophil elastase (Elane)* and *Proteinase 3 (Prtn3)* mRNA in isolated K14-IL-17A<sup>ind/+</sup> neutrophils compared to neutrophils of control mice (Figure 1D). Expression of *Myeloperoxidase (Mpo)* mRNA was also increased in isolated K14-IL-17A<sup>ind/+</sup> neutrophils compared to neutrophils from control mice, whereas there was no difference in *Interleukin-1β (IL-1b)* expression (Figure 1D). These results underscore the increased reactivity of K14-IL-17A<sup>ind/+</sup> neutrophil granulocytes due to the continuous IL-17A exposure.

Next, we set to investigate levels of pro-inflammatory mediators in the skin and aorta of the psoriatic mice. We found increased mRNA expression of the *Chemokine (C-X-C motif) ligand 2 (Cxcl2)* and the *S100 calcium-binding protein A9 (S100a9)* in the skin of K14-IL-17A<sup>ind/+</sup> mice compared to control mice (Figure 2A), two factors that were previously found to contribute to leukocyte recruitment.<sup>40,41</sup> Interestingly, mRNA expression of *Cxcl2* and *S100a9* was not only increased in the skin but also in the aortic tissue of psoriatic animals (Figure 2A). This was in accordance with the previously described invasion of neutrophils into the aortic vessel wall in K14-IL-17A<sup>ind/+</sup> mice parallel to the existing skin inflammation.<sup>23</sup> Moreover, mRNA expression of *Nuclear Factor Erythroid*

*2 Related Factor 2 (Nrf2)*, a transcription factor that regulates protection against oxidative stress,<sup>42</sup> as well as mRNA expression of the antioxidant enzymes *Superoxide dismutase 1, 2 and 3 (Sod1-3)*<sup>43,44</sup> and *Solute Carrier Family 41, Member 3 (Scl41a3)*<sup>45</sup> were not increased, neither in skin, nor in the aorta (Figure 2B,C).

Given the presence of ROS-producing neutrophils in the skin and aorta of K14-IL-17A<sup>ind/+</sup> psoriatic mice,<sup>23</sup> we wanted to investigate whether we could find evidence of a direct interaction between inflamed skin and blood vessels by following a possible migration of inflammatory cells from the psoriatic plaque into the aortic vessel wall. To this end, we crossed the mouse model of K14-IL-17A<sup>ind/+</sup> mice with the *PhAM<sup>excised</sup>* line so that these mice constantly produce the green fluorescent protein Dendra2 in their mitochondria.<sup>31</sup> The color of the Dendra protein changes from green to red fluorescence under laser illumination with a wavelength of 405 nm making it possible to track immune cells from the psoriatic skin (Figure 3A). PhAM-K14-IL-17A<sup>ind/+</sup> mice showed a severe psoriasis-like skin phenotype seen by cumulative PASI score (Figure 3B) as described for the conventional K14-IL-17A<sup>ind/+</sup> mice.<sup>22,23</sup> We therefore exposed 9–10 weeks old PhAM-K14-IL-17A<sup>ind/+</sup> mice to laser light and 24 h later isolated skin, brachial LNs, spleen and aorta for flow cytometric analysis. In line with the severe skin inflammation and previous corroborating reports,<sup>22,23</sup> significantly elevated levels of Gr-1<sup>+</sup> cells in the skin, brachial LNs, spleen and aorta compared to the controls were apparent in the K14-IL-17A<sup>ind/+</sup> model with PhAM background (Figure 4A). This indicates that the PhAM background does not impact on the (skin and systemic) inflammatory phenotype. By flow cytometric gating on Dendra2-red cells (Figure 4B), a higher absolute count of red cells was detectable in skin, brachial LNs and spleen of the illuminated PhAM-K14-IL-17A<sup>ind/+</sup> mice as well as in illuminated PhAM-IL-17A<sup>ind/+</sup> control mice compared to unilluminated animals (Figure 4B,C). However, neither group's aortic vessel wall showed a red cell population (Figure 4B,C). We could therefore exclude a direct cellular trafficking from the skin to the aortic vessel wall. Since the psoriatic skin is not the only source for potentially invading reactive myeloid cells, we also analyzed neutrophil and monocyte numbers in the bone marrow of K14-IL-17A<sup>ind/+</sup> mice compared to controls. Significantly increased values for neutrophils in the bone marrow of K14-IL-17A<sup>ind/+</sup> mice compared to control mice were found and monocytes were increased by trend (Figure 5A,B) as potential and obvious source of the immune cells invading the vasculature underlining the systemic effect of the chronic severe skin disease.

In summary, we tracked immune cells from the psoriatic skin to other tissues, analyzed soluble factors, and

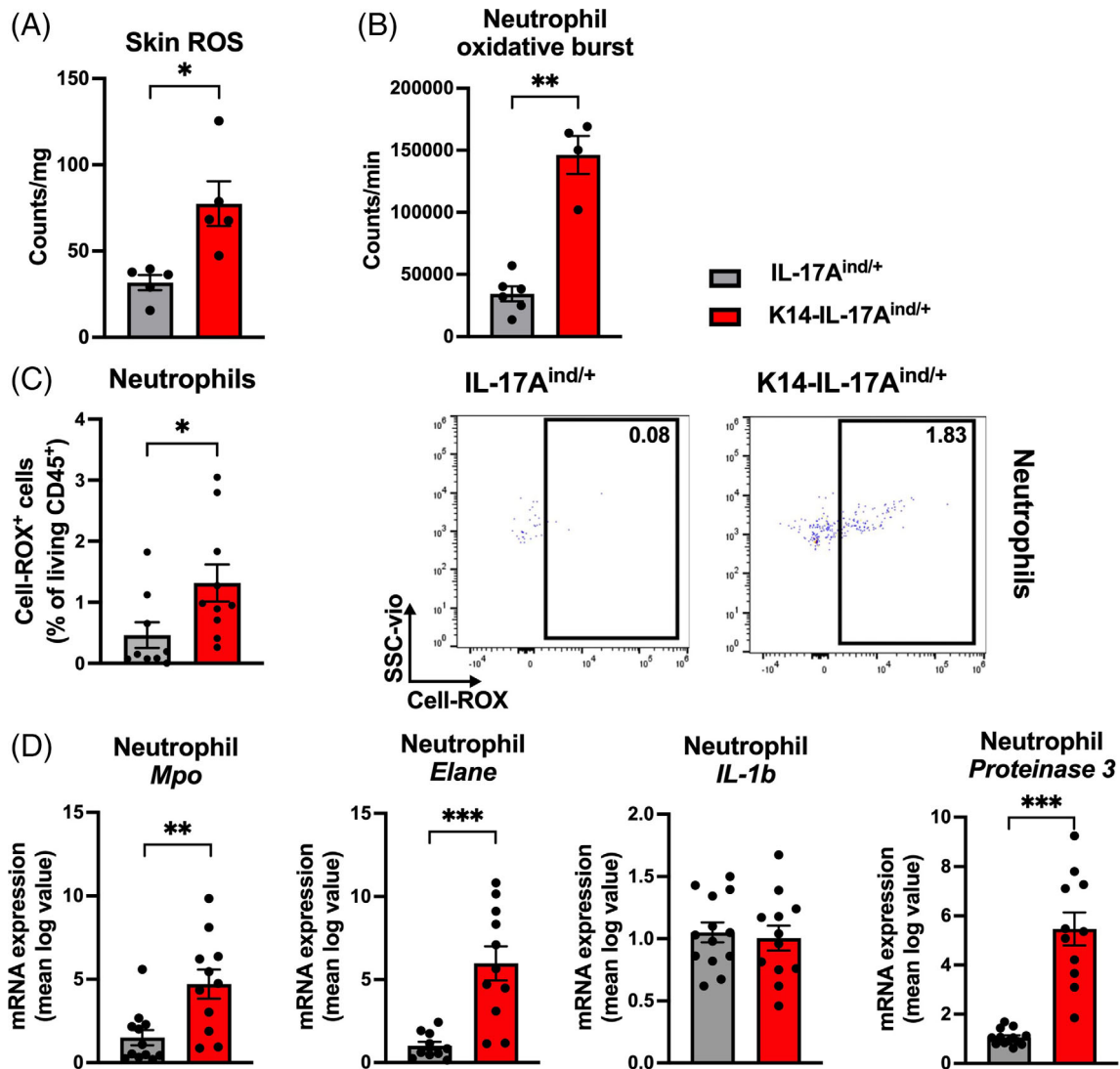


**FIGURE 1** Increased reactive oxygen species (ROS) formation in the psoriatic skin is paralleled by a higher activation. (A) Photometric analysis of superoxide levels in healthy skin of IL-17A<sup>ind/+</sup> mice and in plaque-affected skin of K14-IL-17A<sup>ind/+</sup> mice after incubation with Lucigenin (bis-N-methylacridinium nitrate),  $n = 5$  mice per group, 4 experiments, unpaired Student's *t*-test. (B) Oxidative burst measurement of isolated neutrophils of K14-IL-17A<sup>ind/+</sup> or PhAM-K14-IL-17A<sup>ind/+</sup> mice and controls.  $2.5 \times 10^5$  cells per sample were incubated with PDBu (Phorbol-12,13-dibutyrate) for 10 min at 37°C,  $n = 4$ –6 mice, partially pooled blood samples of three independent experiments, Mann–Whitney test. (C) ROS flow cytometric analysis of living CD45<sup>+</sup> CD11b<sup>+</sup> Ly6G<sup>+</sup> Ly6C<sup>+</sup> neutrophil granulocytes of K14-IL-17A<sup>ind/+</sup> and control mice.  $n = 9$ –10 mice per group, four experiments, Mann–Whitney test. (D) qRT-PCR analysis of neutrophils isolated from the blood of K14-IL-17A<sup>ind/+</sup> or PhAM-K14-IL-17A<sup>ind/+</sup> mice and Cre-negative controls,  $n = 10$ –13 per group, partially pooled blood samples of two independent experiments with 13–16 mice in total, unpaired Student's *t*-test.

ROS. We found an increased reactivity of neutrophils detectable in murine IL-17A driven psoriasis-like skin disease contributing to increased ROS formation in the skin and as previously shown the vasculature.<sup>23</sup> However, ROS-producing myeloid cells did not directly migrate from the inflamed psoriatic plaque to the aortic vessel wall leading us to the conclusion that vascular inflammation in murine IL-17A driven psoriasis-like skin disease is most likely driven by systemic effects of the

chronic inflammatory environment including activated bone marrow.

## 4 | DISCUSSION

The skin-vasculature crosstalk in severe psoriasis leads to cardiovascular comorbidity and is of high clinical importance.<sup>10,21,23,46</sup> When confronted with the associated

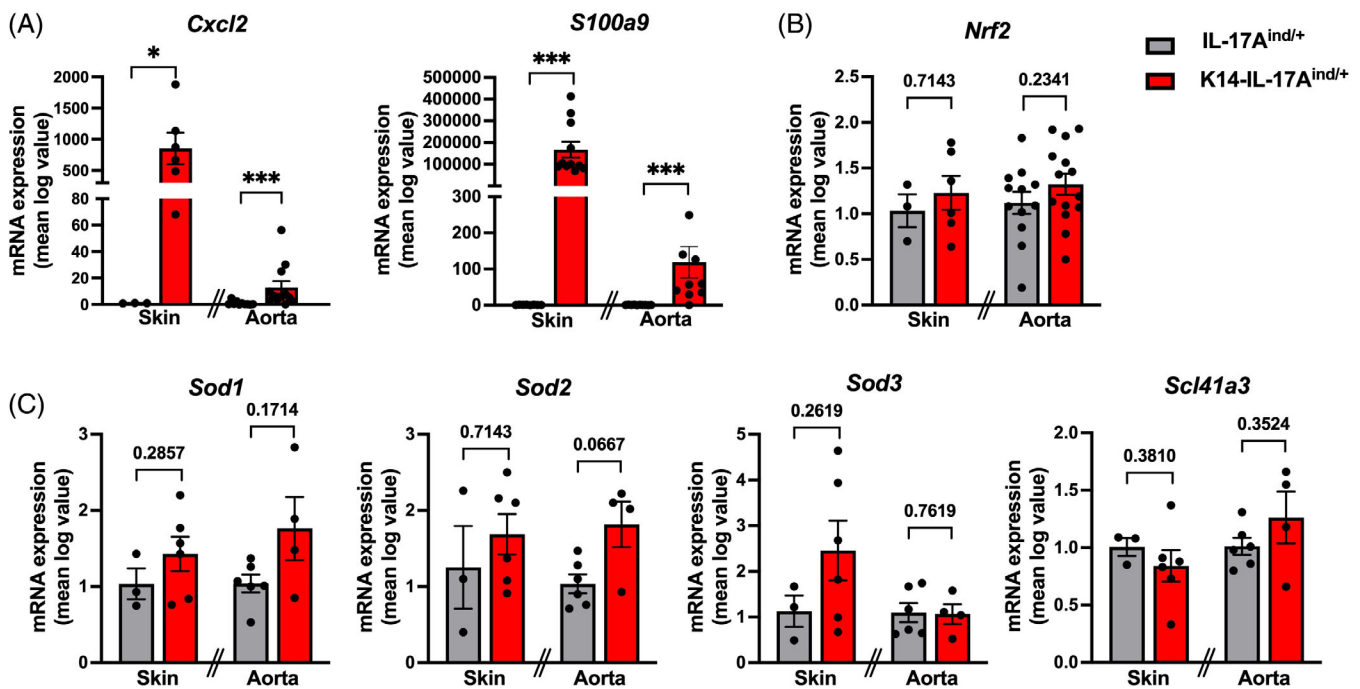


**FIGURE 2** Expression of markers for neutrophil migration or oxidative stress protection in skin and aorta of K14-IL-17A<sup>ind/+</sup> psoriatic mice. (A) Quantitative RT-PCR analysis of *Cxcl2* ( $n(\text{skin}) = 3-6$  and  $n(\text{aorta}) = 10-12$  mice per group; 1-2 independent experiments), *S100a9* ( $n(\text{skin}) = 8-11$ ,  $n(\text{aorta}) = 10$  mice per group; 2 independent experiments) in aorta and skin of K14-IL-17A<sup>ind/+</sup> mice and controls, Mann-Whitney test. (B,C) Quantitative RT-PCR analysis of *Nrf2* ( $n(\text{skin}) = 3-6$ ,  $n(\text{aorta}) = 12-14$  mice per group, 1-2 independent experiments), *Sod1* ( $n(\text{skin}) = 3-6$ ,  $n(\text{aorta}) = 4-6$  mice per group, 1 independent experiment), *Sod2* ( $n(\text{skin}) = 3-6$ ,  $n(\text{aorta}) = 4-6$ , 1 independent experiment), *Sod3* ( $n(\text{skin}) = 3-6$ ,  $n(\text{aorta}) = 4-6$ , 1 independent experiment) and *Scl41a3* ( $n(\text{skin}) = 3-6$ ,  $n(\text{aorta}) = 4-6$ , 1 independent experiment) in aorta and skin of K14-IL-17A<sup>ind/+</sup> mice and controls, Mann-Whitney or unpaired Student's *t*-test (*Nrf2* in aorta). Data is presented as mean  $\pm$  SEM. \*\*\* $P < 0.001$ ; \*\* $P < 0.01$ ; \* $P < 0.05$ .

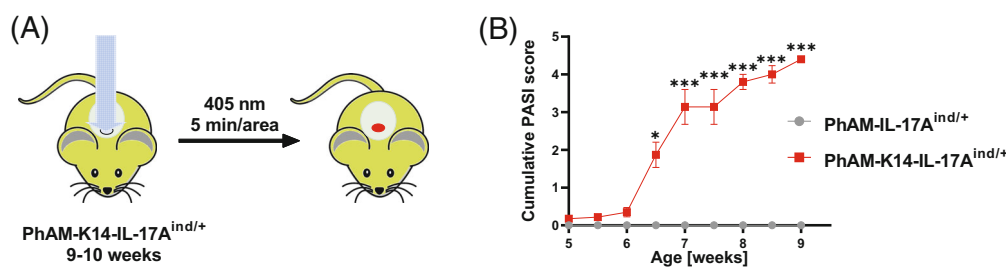


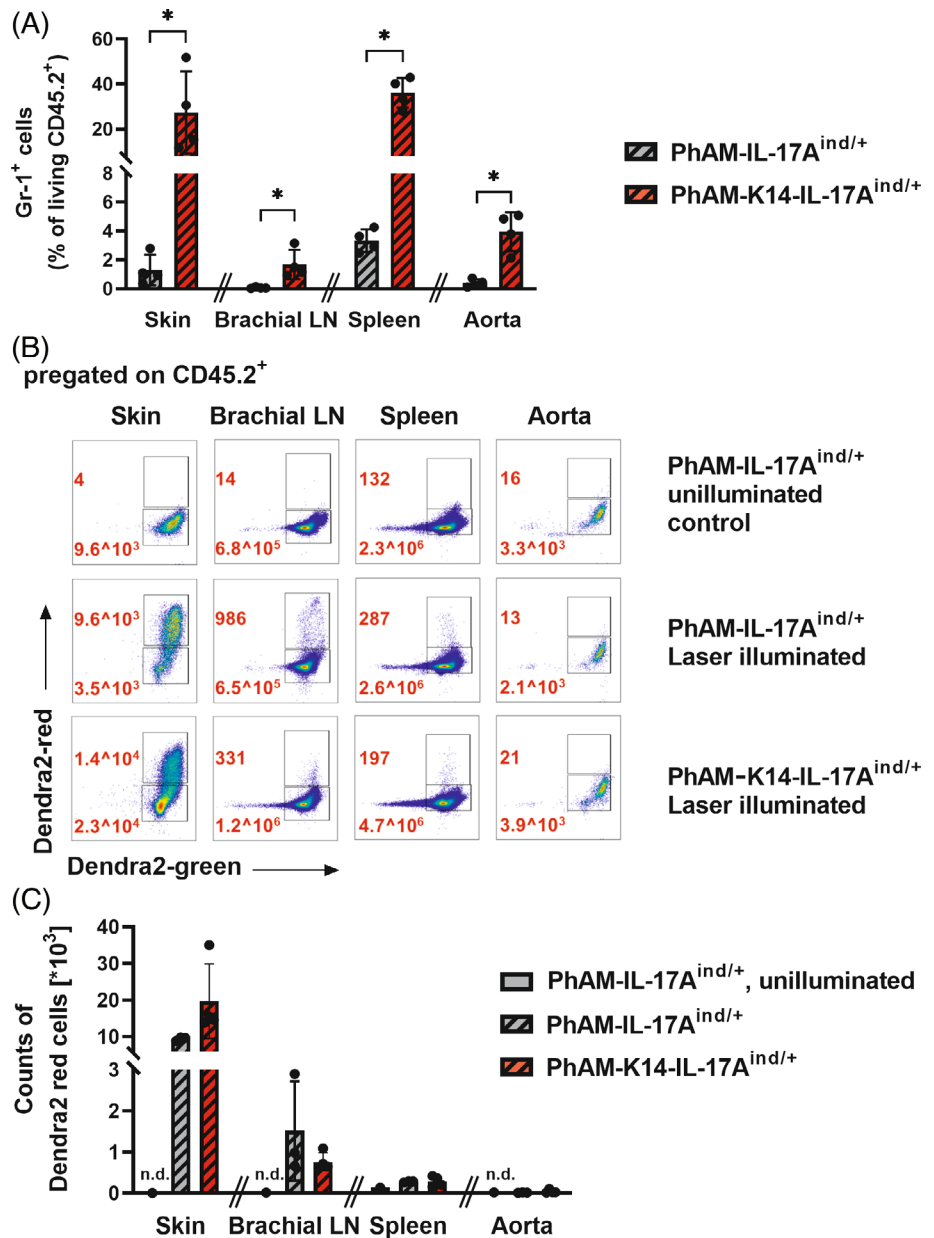
**FIGURE 3** Schematic illustration of experimental procedure for cell tracking with PhAM-K14-IL-17A<sup>ind/+</sup> psoriasis mouse model. (A) Illustration of the experimental procedure for photoconverting green-fluorescing Dendra2 into red-fluorescence using a 405 nm laser on the psoriatic plaque. (B) Cumulative PASI-scores of PhAM-K14-IL-17A<sup>ind/+</sup> and PhAM-IL-17A<sup>ind/+</sup> mice are shown consisting of erythema and scaling scores multiplied by affected area [%] ([erythema score + scaling score]  $\times$  affected area [%]/100),  $n = 4$  mice per group, 1 representative experiment, 2-way ANOVA with Bonferroni post hoc test.

cardiovascular comorbidity in psoriasis, the main question is: How are both diseases interconnected? Meanwhile, it has been recognized that severe psoriasis is an independent cardiovascular risk factor.<sup>10</sup> In 2011, the systemic inflammation in severe psoriasis was assumed to be one relevant connecting factor between skin inflammation and vascular dysfunction.<sup>47</sup> Nowadays, we know much more about cytokines such as IL-17A and tumor

necrosis factor alpha (TNF- $\alpha$ ) contributing to vascular inflammation and dysfunction, thus paving the way for the interconnecting skin and vessel inflammation in psoriasis.<sup>23,48,49</sup> We have previously demonstrated that the psoriasis-like skin inflammation in K14-IL-17A<sup>ind/+</sup> psoriatic mice was accompanied by vascular inflammation, specifically by invasion of neutrophil granulocytes into the aortic vessel wall combined with increased aortic



**FIGURE 4** Tracking of skin-derived immune cells in the PhAM-K14-IL-17A<sup>ind/+</sup> psoriasis mouse model shows no inflammatory cells migrating from the inflamed skin into the vasculature. (A) Flow cytometric analysis of Gr-1<sup>+</sup> cells in the skin, brachial lymph nodes (LNs), spleen, and aorta of PhAM-K14-IL-17A<sup>ind/+</sup> mice compared to Cre-negative PhAM-IL-17A<sup>ind/+</sup> mice. Cells were pre-gated on living CD45.2<sup>+</sup> cells,  $n = 4$  mice per group, 1 individual experiment, Mann-Whitney test. (B) One representative flow cytometry plot pre-gated on living CD45.2<sup>+</sup> cells is shown per organ and group of 6 experiments. Cell counts of the gates are shown. (C) Laser illuminated PhAM-K14-IL-17A<sup>ind/+</sup> and PhAM-IL-17A<sup>ind/+</sup> mice and unilluminated control were analyzed for red-fluorescing mito-Dendra2 cells via flow cytometry. Counts of red-fluorescing (Dendra2-red) living CD45.2<sup>+</sup> cells for skin, brachial LN, spleen and aorta calculated for the whole organ are shown,  $n = 3-4$  mice per group plus one unilluminated background control, 1 representative experiment of 6 individual experiments, Mann-Whitney test. n.d., not determinable.



ROS formation.<sup>23</sup> This is in line with reports of vascular inflammation in human psoriasis patients<sup>24</sup> and contributes to the cardiovascular comorbidity found in severe psoriasis. This study demonstrates increased reactivity and ROS production of neutrophils in K14-IL-17A<sup>ind/+</sup> psoriatic mice most likely due to the continuous IL-17A stimulation. Both ROS levels in the skin and the neutrophilic oxidative burst were detected by lucigenin and luminol assays, respectively.<sup>50,51</sup> The lucigenin electrochemiluminescence method has previously been compared to other superoxide detection methods and tested by specific inhibition, revealing a good correlation with other methods of superoxide detection.<sup>52-54</sup>

Notwithstanding, these methods can be associated with artifacts.<sup>50</sup> Besides, the clear detection of O<sub>2</sub><sup>•-</sup>

remains vague, but it can be used as general indicator of increased ROS production.<sup>51</sup> Increased ROS formation in neutrophils of K14-IL-17A<sup>ind/+</sup> psoriatic mice compared to control mice was also confirmed by flow cytometric analysis. Taken together, our data indicate a generally increased ROS formation in the skin associated with higher neutrophil activation in K14-IL-17A<sup>ind/+</sup> psoriatic mice. In future, additional methods to quantify oxidative damage markers induced by neutrophils in autoimmune diseases will be needed to corroborate these data. In accordance with increased ROS formation, we did not find significantly increased levels of *Nrf2* and of the downstream targets of *Nrf2* such as *Superoxide dismutases 1-3 (Sod1-3)*<sup>43,44</sup> and *Solute Carrier Family 41, Member 3 (Scl41a3)*<sup>45</sup> on mRNA expression level in skin and aorta. The

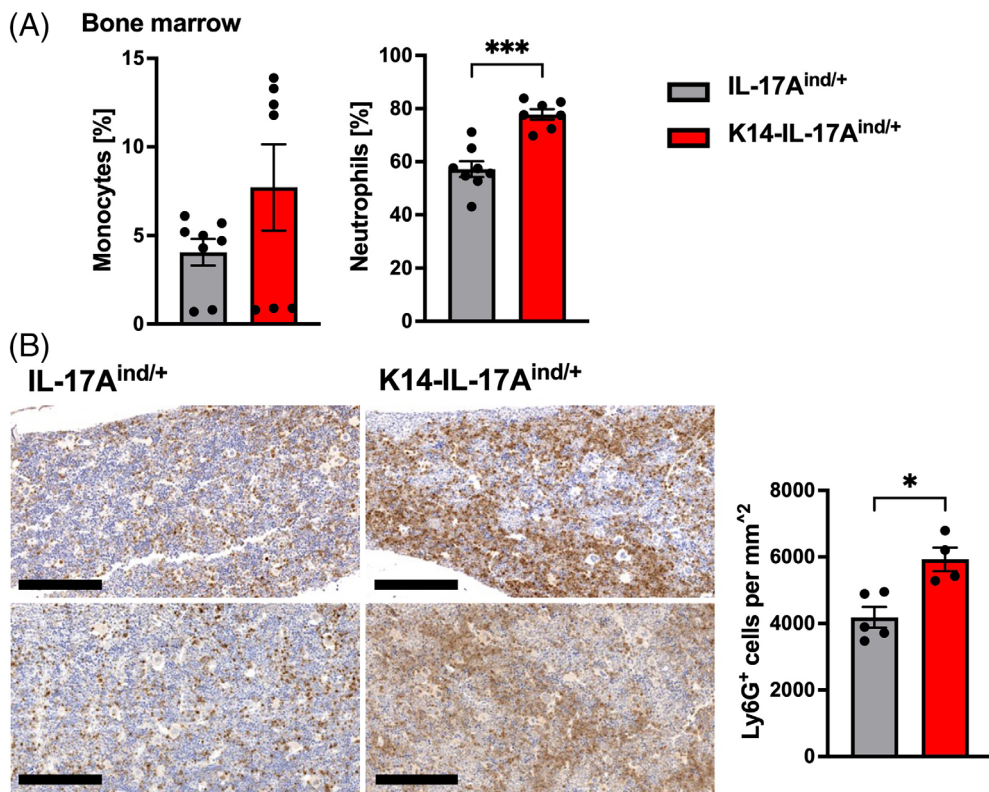


**FIGURE 5** Analysis of monocytes and neutrophils in the bone marrow of K14-IL-17A<sup>ind/+</sup> mice. (A) Percentages of monocytes or neutrophils in the bone marrow of K14-IL-17A<sup>ind/+</sup> mice and Cre-negative littermates analyzed via VetScan HM5,  $n = 7-8$  mice per group, four individual experiments, Mann-Whitney test (monocytes) and unpaired Student's *t*-test (neutrophils). (B) Ly6G staining and quantification on bone marrow paraffin sections of IL-17A<sup>ind/+</sup> and K14-IL-17A<sup>ind/+</sup> mice.  $n = 4-5$ , scale bar: 200  $\mu\text{m}$ . Data were analyzed with Mann-Whitney test. Data are shown as mean  $\pm$  SEM. \*\*\* $P < 0.001$ ; \*\* $P < 0.01$ ; \* $P < 0.05$ .

transcription factor Nrf2 is considered a central regulator of cellular defense mechanisms against oxidative stress.<sup>42</sup> One might speculate that in our murine model of psoriasis the anti-oxidant system associated with Nrf2 is mainly inactive or not fully activated, possibly thus contributing to the increased ROS formation detected in the aorta<sup>23</sup> and skin.

Further detailed analysis of the Nrf2 activation state, expression of downstream targets, as well as nuclear fraction extraction to investigate phosphorylation on Ser40 of Nrf2 (responsible for translocation into the nucleus)<sup>55</sup> providing a better insight into the Nrf2 activity have to follow in the K14-IL-17A<sup>ind/+</sup> psoriatic mice. Up to now, data on Nrf2 in psoriasis patients is controversial: Upregulated mRNA levels of *Nrf2* were detected in the skin of psoriasis patients<sup>56</sup> but in another patient cohort also a reduced dermal *Nrf2* expression was described in psoriasis vulgaris.<sup>57</sup> Further studies with more patients also focusing on gender differences<sup>58,59</sup> as well as the severity of skin disease need to follow to gain further insights in the role of Nrf2 in psoriasis.

However, we must be aware that besides the inflammatory skin vasculature crosstalk, severe psoriasis is associated with extensive water loss via the inflamed skin leading to compensatory mechanisms associated with arterial hypertension which vice versa contributes to the cardiovascular risk profile.<sup>60</sup> Overall, we are faced with a multi-dimensional and highly complex problem.

The pro-inflammatory protein S100a9 is upregulated in the skin of psoriasis patients and psoriatic-like mouse models<sup>61,62</sup> activating the inflammatory response in innate immune cells via TLR4-dependent signaling.<sup>63,64</sup> The increased *Cxcl2* and *S100a9* mRNA expression in the skin and the aorta of K14-IL-17A<sup>ind/+</sup> compared to control mice might indicate that there are similar neutrophil recruiting mechanisms in both the skin and the vasculature. In steady state *neutrophil elastase* and *proteinase 3* reside inside the granules of neutrophils and are released to the environment only upon activation.<sup>65</sup> Therefore, these serine proteinases' upregulated mRNA level state in the K14-IL-17A<sup>ind/+</sup> mice might hint towards an enhanced neutrophilic activity.

Interestingly, there was no direct migration of myeloid cells from the inflamed skin into the vasculature detectable in the PhAM-K14-IL-17A<sup>ind/+</sup> mice, displaying the psoriatic phenotype previously described for the K14-IL-17A<sup>ind/+</sup> mice combined with the possibility to directly track cells.<sup>23,31</sup> The irreversibility of the photo-conversion reaction of Dendra2 from green to red makes the PhAM system very robust.<sup>66</sup> Previous *in vivo* studies successfully used the PhAM system for immune cell tracking in other disease models detecting converted cells after 24 h and even after 3 days.<sup>67,68</sup>

Similar to the murine model of Angiotensin II driven vascular dysfunction and hypertension which is based on the invasion of ROS-producing myeloid cells into the

vessel wall,<sup>19</sup> our murine model of severe psoriasis concomitant with vascular dysfunction is associated with vascular inflammation especially based on the influx of ROS producing neutrophils to the vessel walls.<sup>23</sup> In both models, ROS-producing myeloid cells are most likely bone marrow derived, as indicated by increased levels of neutrophils and monocytes in the bone marrow of K14-IL-17A<sup>ind/+</sup> mice compared to controls. This highlights the systemic components of vascular and psoriatic skin disease. The systemic character of severe psoriatic inflammation must be kept in mind when treating psoriasis patients, as it is responsible for most relevant comorbidities highlighting the importance of a multidimensional treatment approach.

### AUTHOR CONTRIBUTIONS

Theresa Schaller and Julia Ringen performed experiments, analyzed data, and performed statistical analysis. Berenice Fischer, Tabea Bieler, and Katharina Perius performed experiments and analyzed data. Tanja Knopp, Katharina S. Kommos, Thomas Münzel, and Philip Wenzel supported the project with valuable discussions, technical, and scientific experience and supervision, and the critical reading of the manuscript. Thomas Korn provided the PhAM<sup>excised</sup> mouse model and the experience with these mice. Mathias Heikenwälder, Matthias Oelze, Andreas Daiber, and Daniela Kramer provided methods, material, supervision of experiments and valuable discussions. Susanne Karbach, Johannes Wild, and Ari Waisman acquired funding, designed the study, and directed the experimental work. Susanne Karbach developed the concept and Susanne Karbach, Johannes Wild, and Ari Waisman supervised experiments and wrote the manuscript.

### ACKNOWLEDGMENTS

We thank Angelica Karpi for excellent technical help and support. Thanks to Annika Lehmann for proofreading and to Rebecca Jung for continuous fruitful discussion. Open Access funding enabled and organized by Projekt DEAL.

### FUNDING INFORMATION

This study was funded by the Boehringer Ingelheim Foundation “Novel and neglected cardiovascular risk factors: molecular mechanisms and therapeutic implications” (Susanne Karbach, Johannes Wild, Philip Wenzel, and Thomas Münzel) and by the Deutsche Forschungsgemeinschaft (DFG) TRR 156/2 (ID 246807620, Katharina S. Kommos, Susanne Karbach, Ari Waisman, Daniela Kramer). Tabea Bieler received funding from the Federal Ministry of Education and Research (BMBF) and the Ministry of Science Baden-Württemberg within the framework of the Excellence Strategy of Germany’s Federal and State Governments. Katharina S. Kommos is

funded by the Physician-Scientist Program of Heidelberg University, Faculty of Medicine. Johannes Wild is supported by the German Federal Ministry for Education and Research (BMBF EDU-V24) and the University of Mainz (“Inneruniversitäre Forschungsförderung”). Susanne Karbach was supported by the German Research Foundation (DFG KA 4035/1-1). Susanne Karbach and Philip Wenzel received funding by the Federal Ministry of Education and Research (BMBF 01EO1503) related to this study. Susanne Karbach is funded by the Deutsche Herzstiftung and by the DZHK Excellence Program (“Interleukin-17A mediated inflammation in myocardial infarction in a mouse model of psoriasis-like skin disease.”). Ari Waisman and Thomas Korn were supported by the DFG via project 490846870 TRR355/1. Daniela Kramer is funded by Else-Kröner-Fresenius and the Peter-Hans Hofschneider Foundation. Thomas Korn was supported by the DFG (SFB1054 [ID 210592381], TRR128 [ID 213904703], TRR274 [ID 408885537], TRR355 [ID 490846870], EXC 2145 [SyNergy, ID 390857198]), and by the Hertie Network of Clinical Neuroscience.

### CONFLICT OF INTEREST STATEMENT

Susanne Karbach declares having received consultancy honoraria from Admiral and lecture honoraria from Janssen-Cilag. The other authors declare no conflicts of interest.

### DATA AVAILABILITY STATEMENT

The data that support the findings of this study are available from the corresponding author upon reasonable request. The data are stored on the server of the Center for Thrombosis and Hemostasis (CTH), University Medical Center of the Johannes Gutenberg University Mainz. The graphical abstract was adapted from the BioRender template “The IL-23/IL-17 Axis in Psoriasis” with BioRender.com (2022). Retrieved from <https://app.biorender.com/biorender-templates>.

### ORCID


Theresa Schaller  <https://orcid.org/0000-0002-1208-7823>

Julia Ringen  <https://orcid.org/0000-0002-8488-6376>

Tabea Bieler  <https://orcid.org/0000-0003-3611-9305>

Katharina S. Kommos  <https://orcid.org/0000-0003-2428-2658>

Johannes Wild  <https://orcid.org/0000-0002-1446-8101>

Susanne Karbach  <https://orcid.org/0000-0003-4462-3747>

Ari Waisman  <https://orcid.org/0000-0003-4304-8234>

### REFERENCES

1. Lowes MA, Suarez-Farinas M, Krueger JG. Immunology of psoriasis. *Annu Rev Immunol*. 2014;32:227–55.

2. Griffiths CEM, Armstrong AW, Gudjonsson JE, Barker J. Psoriasis. *Psoriasis Lancet*. 2021;397:1301–15.
3. Global Burden of Disease Collaborative Network. Global burden of disease study 2010 (GBD 2010) results by cause 1990–2010. Seattle, WA: Institute for Health Metrics and Evaluation (IHME); 2012.
4. Hay RJ, Johns NE, Williams HC, Bolliger IW, Dellavalle RP, Margolis DJ, et al. The global burden of skin disease in 2010: an analysis of the prevalence and impact of skin conditions. *J Invest Dermatol*. 2014;134:1527–34.
5. Bocheńska K, Smolińska E, Moskot M, Jakóbkiewicz-Banecka J, Gabig-Cimińska M. Models in the research process of psoriasis. *Int J Mol Sci*. 2017;18:2514.
6. Brembilla NC, Senra L, Boehncke W-H. The IL-17 family of cytokines in psoriasis: IL-17A and beyond. *Front Immunol*. 2018;9:1682.
7. Di Meglio P, Villanova F, Nestle FO. Psoriasis. *Cold Spring Harb Perspect Med*. 2014;4.
8. Griffiths CE, Barker JN. Pathogenesis and clinical features of psoriasis. *Lancet*. 2007;370:263–71.
9. Yamazaki F. Psoriasis: Comorbidities. *J Dermatol*. 2021;48:732–40.
10. Mehta NN, Azfar RS, Shin DB, Neimann AL, Troxel AB, Gelfand JM. Patients with severe psoriasis are at increased risk of cardiovascular mortality: cohort study using the general practice research database. *Eur Heart J*. 2010;31:1000–6.
11. Vena GA, Vestita M, Cassano N. Psoriasis and cardiovascular disease. *Dermatol Ther*. 2010;23:144–51.
12. Martin DA, Towne JE, Kricorian G, Klekotka P, Gudjonsson JE, Krueger JG, et al. The emerging role of IL-17 in the pathogenesis of psoriasis: preclinical and clinical findings. *J Invest Dermatol*. 2013;133:17–26.
13. Song X, Qian Y. IL-17 family cytokines mediated signaling in the pathogenesis of inflammatory diseases. *Cell Signal*. 2013; 25:2335–47.
14. Boehncke W-H, Schoen MP. Psoriasis. *Lancet*. 2015;386: 983–94.
15. Mizuguchi S, Gotoh K, Nakashima Y, Setoyama D, Takata Y, Ohga S, et al. Mitochondrial reactive oxygen species are essential for the development of psoriatic inflammation. *Front Immunol*. 2021;12:714897.
16. Zhang Y, Li Y, Zhou L, Yuan X, Wang Y, Deng Q, et al. Nav1.8 in keratinocytes contributes to ROS-mediated inflammation in inflammatory skin diseases. *Redox Biol*. 2022;55:102427.
17. Forstermann U, Munzel T. Endothelial nitric oxide synthase in vascular disease: from marvel to menace. *Circulation*. 2006; 113:1708–14.
18. Woollard KJ, Geissmann F. Monocytes in atherosclerosis: subsets and functions. *Nat Rev Cardiol*. 2010;7:77–86.
19. Wenzel P, Knorr M, Kossmann S, Stratmann J, Hausding M, Schuhmacher S, et al. Lysozyme M-positive monocytes mediate angiotensin II-induced arterial hypertension and vascular dysfunction. *Circulation*. 2011;124:1370–81.
20. Wantha S, Alard JE, Megens RT, van der Does AM, Doring Y, Drechsler M, et al. Neutrophil-derived cathelicidin promotes adhesion of classical monocytes. *Circ Res*. 2013;112:792–801.
21. Orlando G, Molon B, Viola A, Alaibac M, Angioni R, Piaserico S. Psoriasis and cardiovascular diseases: an immune-mediated cross talk? *Front Immunol*. 2022;13:868277.
22. Croxford AL, Karbach S, Kurschus FC, Wörtge S, Nikolaev A, Yogeve N, et al. IL-6 regulates neutrophil microabscess formation in IL-17A-driven psoriasiform lesions. *J Invest Dermatol*. 2014;134:728–35.
23. Karbach S, Croxford AL, Oelze M, Schüler R, Minwegen D, Wegner J, et al. Interleukin 17 drives vascular inflammation, endothelial dysfunction, and arterial hypertension in psoriasis-like skin disease. *Arterioscler Thromb Vasc Biol*. 2014;34: 2658–68.
24. Mehta NN, Yu Y, Saboury B, Foroughi N, Krishnamoorthy P, Raper A, et al. Systemic and vascular inflammation in patients with moderate to severe psoriasis as measured by [18F]-fluorodeoxyglucose positron emission tomography-computed tomography (FDG-PET/CT): a pilot study. *Arch Dermatol*. 2011;147:1031–9.
25. Elnabawi YA, Dey AK, Goyal A, Groenendyk JW, Chung JH, Belur AD, et al. Coronary artery plaque characteristics and treatment with biologic therapy in severe psoriasis: results from a prospective observational study. *Cardiovasc Res*. 2019;115:721–8.
26. Elnabawi YA, Oikonomou EK, Dey AK, Mancio J, Rodante JA, Aksentijevich M, et al. Association of Biologic Therapy with coronary Inflammation in patients with psoriasis as assessed by perivascular fat attenuation index. *JAMA Cardiol*. 2019;4: 885–91.
27. Schüler R, Brand A, Klebow S, Wild J, Veras FP, Ullmann E, et al. Antagonization of IL-17A attenuates skin inflammation and vascular dysfunction in mouse models of psoriasis. *J Invest Dermatol*. 2019;139:638–47.
28. Barbieri JS, Beidas RS, Gondo GC, Fishman J, Williams NJ, Armstrong AW, et al. Analysis of specialist and patient perspectives on strategies to improve cardiovascular disease prevention among persons with psoriatic disease. *JAMA Dermatol*. 2022;158:252–9.
29. Garshick MS, Berger JS. Psoriasis and cardiovascular disease—an ounce of prevention is worth a pound of cure. *JAMA Dermatol*. 2022;158:239–41.
30. Hafner M, Wenk J, Nenci A, Pasparakis M, Scharffetter-Kochanek K, Smyth N, et al. Keratin 14 Cre transgenic mice authenticate keratin 14 as an oocyte-expressed protein. *Genesis*. 2004;38:176–81.
31. Pham AH, McCaffery JM, Chan DC. Mouse lines with photo-activatable mitochondria to study mitochondrial dynamics. *Genesis*. 2012;50:833–43.
32. Cossarizza A, Chang HD, Radbruch A, Acs A, Adam D, Adam-Klages S, et al. Guidelines for the use of flow cytometry and cell sorting in immunological studies (second edition). *Eur J Immunol*. 2019;49:1457–973.
33. Oelze M, Daiber A, Brandes RP, Hortmann M, Wenzel P, Hink U, et al. Nebivolol inhibits superoxide formation by NADPH oxidase and endothelial dysfunction in angiotensin II-treated rats. *Hypertension*. 2006;48:677–84.
34. Daiber A, August M, Baldus S, Wendt M, Oelze M, Sydow K, et al. Measurement of NAD (P) H oxidase-derived superoxide with the luminol analogue L-012. *Free Rad Biol Med*. 2004;36:101–11.
35. Zielonka J, Lambeth JD, Kalyanaraman B. On the use of L-012, a luminol-based chemiluminescent probe, for detecting superoxide and identifying inhibitors of NADPH oxidase: a reevaluation. *Free Rad Biol Med*. 2013;65:1310–4.



36. Du E, Ha S, Diez-Silva M, Dao M, Suresh S, Chandrakasan AP. Electric impedance microflow cytometry for characterization of cell disease states. *Lab Chip*. 2013;13:3903–9.
37. Toni LS, Garcia AM, Jeffrey DA, Jiang X, Stauffer BL, Miyamoto SD, Sucharov CC. Optimization of phenol-chloroform RNA extraction. *MethodsX*. 2018;5:599–608.
38. Schuler R, Efentakis P, Wild J, Lagrange J, Garlapati V, Molitor M, et al. T Cell-Derived IL-17A Induces Vascular Dysfunction via Perivascular Fibrosis Formation and Dysregulation of (.)NO/cGMP Signaling. *Oxid Med Cell Longev*. 2019; 6721531.
39. Bankhead P, Loughrey MB, Fernandez JA, Dombrowski Y, McArt DG, Dunne PD, et al. QuPath: open source software for digital pathology image analysis. *Sci Rep*. 2017;7:16878.
40. Croce K, Gao H, Wang Y, Mooroka T, Sakuma M, Shi C, et al. Myeloid-related protein-8/14 is critical for the biological response to vascular injury. *Circulation*. 2009;120:427–36.
41. De Filippo K, Dudeck A, Hasenberg M, Nye E, van Rooijen N, Hartmann K, et al. Mast cell and macrophage chemokines CXCL1/CXCL2 control the early stage of neutrophil recruitment during tissue inflammation. *Blood*. 2013;121:4930–7.
42. Dodson M, de la Vega MR, Cholanians AB, Schmidlin CJ, Chapman E, Zhang DD. Modulating NRF2 in disease: timing is everything. *Annu Rev Pharmacol Toxicol*. 2019;59:555–75.
43. Michiels C, Raes M, Toussaint O, Remacle J. Importance of S-glutathione peroxidase, catalase, and Cu/Zn-SOD for cell survival against oxidative stress. *Free Radic Biol Med*. 1994;17: 235–48.
44. Nguyen NH, Tran GB, Nguyen CT. Anti-oxidative effects of superoxide dismutase 3 on inflammatory diseases. *J Mol Med (Berl)*. 2020;98:59–69.
45. Fleig A, Schweigel-Rontgen M, Kolisek M. Solute carrier family SLC41, what do we really know about it? *Wiley Interdiscip rev Membr Trans Signal*. 2013;2:227–239.
46. Conrad N, Verbeke G, Molenberghs G, Goetschalckx L, Callender T, Cambridge G, et al. Autoimmune diseases and cardiovascular risk: a population-based study on 19 autoimmune diseases and 12 cardiovascular diseases in 22 million individuals in the UK. *Lancet*. 2022;400:733–43.
47. Boehncke WH, Boehncke S, Tobin AM, Kirby B. The 'psoriatic march': a concept of how severe psoriasis may drive cardiovascular comorbidity. *Exp Dermatol*. 2011;20:303–7.
48. Madhur MS, Lob HE, McCann LA, Iwakura Y, Blinder Y, Guzik TJ, et al. Interleukin 17 promotes angiotensin II-induced hypertension and vascular dysfunction. *Hypertension*. 2010;55:500–7.
49. Mehta NN, Teague HL, Swindell WR, Baumer Y, Ward NL, Xing X, et al. IFN-gamma and TNF-alpha synergism may provide a link between psoriasis and inflammatory atherogenesis. *Sci Rep*. 2017;7:13831.
50. Munzel T, Afanas'ev IB, Kleschyov AL, Harrison DG. Detection of superoxide in vascular tissue. *Arterioscler Thromb Vasc Biol*. 2002;22:1761–8.
51. Murphy MP, Bayir H, Belousov V, Chang CJ, Davies KJA, Davies MJ, et al. Guidelines for measuring reactive oxygen species and oxidative damage in cells and in vivo. *Nat Metab*. 2022;4:651–62.
52. Kroller-Schon S, Steven S, Kossmann S, Scholz A, Daub S, Oelze M, et al. Molecular mechanisms of the crosstalk between mitochondria and NADPH oxidase through reactive oxygen species-studies in white blood cells and in animal models. *Antioxid Redox Signal*. 2014;20:247–66.
53. Steven S, Daiber A, Dopheide JF, Munzel T, Espinola-Klein C. Peripheral artery disease, redox signaling, oxidative stress—basic and clinical aspects. *Redox Biol*. 2017;12:787–97.
54. Gollner M, Ihrig-Biedert I, Petermann V, Saurin S, Oelze M, Kroller-Schon S, et al. NOX2ko mice show largely increased expression of a mutated NOX2 mRNA encoding an inactive NOX2 protein. *Antioxidants (Basel)*. 2020;9:1043.
55. Huang HC, Nguyen T, Pickett CB. Phosphorylation of Nrf2 at Ser-40 by protein kinase C regulates antioxidant response element-mediated transcription. *J Biol Chem*. 2002;277: 42769–74.
56. Yang L, Fan X, Cui T, Dang E, Wang G. Nrf2 promotes keratinocyte proliferation in psoriasis through up-regulation of keratin 6, keratin 16, and keratin 17. *J Invest Dermatol*. 2017;137: 2168–76.
57. Lee YJ, Bae JH, Kang SG, Cho SW, Chun DI, Nam SM, et al. Pro-oxidant status and Nrf2 levels in psoriasis vulgaris skin tissues and dimethyl fumarate-treated HaCaT cells. *Arch Pharm Res*. 2017;40:1105–16.
58. Lesuis N, Befrits R, Nyberg F, van Vollenhoven RF. Gender and the treatment of immune-mediated chronic inflammatory diseases: rheumatoid arthritis, inflammatory bowel disease and psoriasis: an observational study. *BMC Med*. 2012;10:82.
59. Hagg D, Sundstrom A, Eriksson M, Schmitt-Egenolf M. Severity of psoriasis differs between men and women: a study of the clinical outcome measure psoriasis area and severity index (PASI) in 5438 Swedish register patients. *Am J Clin Dermatol*. 2017;18:583–90.
60. Wild J, Jung R, Knopp T, Efentakis P, Benaki D, Grill A, et al. Aestivation motifs explain hypertension and muscle mass loss in mice with psoriatic skin barrier defect. *Acta Physiol (Oxf)*. 2021;232:e13628.
61. Semprini S, Capon F, Tacconelli A, Giardina E, Orecchia A, Mingarelli R, et al. Evidence for differential S100 gene overexpression in psoriatic patients from genetically heterogeneous pedigrees. *Hum Genet*. 2002;111:310–3.
62. Schonthaler HB, Guinea-Viniegra J, Wculek SK, Ruppen I, Ximenez-Embun P, Guio-Carrion A, et al. S100A8-S100A9 protein complex mediates psoriasis by regulating the expression of complement factor C3. *Immunity*. 2013;39:1171–81.
63. Vogl T, Tenbrock K, Ludwig S, Leukert N, Ehrhardt C, van Zoelen MA, et al. Mrp8 and Mrp14 are endogenous activators of toll-like receptor 4, promoting lethal, endotoxin-induced shock. *Nat Med*. 2007;13:1042–9.
64. Fassl SK, Austermann J, Papantonopoulou O, Riemenschneider M, Xue J, Bertheloot D, et al. Transcriptome assessment reveals a dominant role for TLR4 in the activation of human monocytes by the alarmin MRP8. *J Immunol*. 2015;194:575–83.
65. Korkmaz B, Horwitz MS, Jenne DE, Gauthier F. Neutrophil elastase, proteinase 3, and cathepsin G as therapeutic targets in human diseases. *Pharmacol Rev*. 2010;62: 726–59.
66. Adam V, Nienhaus K, Bourgeois D, Nienhaus GU. Structural basis of enhanced photoconversion yield in green fluorescent protein-like protein Dendra2. *Biochemistry*. 2009;48: 4905–15.

67. Jarick KJ, Mokhtari Z, Scheller L, Hartweg J, Thusek S, Le DD, et al. Photoconversion of Alloreactive T cells in murine Peyer's patches during acute graft-versus-host disease: tracking the homing route of highly proliferative cells in vivo. *Front Immunol.* 2018;9:1468.
68. Hiltensperger M, Beltran E, Kant R, Tyystjarvi S, Lepennetier G, Dominguez Moreno H, et al. Skin and gut imprinted helper T cell subsets exhibit distinct functional phenotypes in central nervous system autoimmunity. *Nat Immunol.* 2021;22:880–92.

**How to cite this article:** Schaller T, Ringen J, Fischer B, Bieler T, Perius K, Knopp T, et al. Reactive oxygen species produced by myeloid cells in psoriasis as a potential biofactor contributing to the development of vascular inflammation. *BioFactors.* 2023;49(4):861–74. <https://doi.org/10.1002/biof.1949>